

## Original Article

# MicroRNA-608 inhibits the cell proliferation in osteosarcoma by macrophage migration inhibitory factor

Jianyue Wu<sup>1\*</sup>, Jianfei Sun<sup>1\*</sup>, Jun Gu<sup>1</sup>, Gonglian Liu<sup>2</sup>, Huizhu Song<sup>2</sup>

<sup>1</sup>Department of Orthopaedics, Wuxi Xishan People's Hospital, Wuxi 214023, China; <sup>2</sup>Department of Pharmacy, Wuxi People's Hospital Affiliated to Nanjing Medical University, Wuxi 214023, China. \*Equal contributors.

Received January 19, 2016; Accepted July 19, 2016; Epub September 1, 2016; Published September 15, 2016

**Abstract:** Osteosarcoma (OS) is the most prevalent malignant bone tumour with high morbidity in children and adolescents. Increasing evidence indicates that microRNAs (miRNAs) play essential roles in OS occurrence and progression. This study aimed to investigate the expression and biological role of microRNA-608 (miR-608) in OS. Here, we found that miR-608 expression was consistently downregulated in OS tissues compared with the matched adjacent normal tissues, and its expression was significantly correlated with overall ( $P=0.0247$ ) and disease-free survival rate ( $P=0.0107$ ), tumour size ( $P=0.0004$ ) and Tumour Node Metastasis (TNM) stage ( $P=0.0005$ ). Functional study revealed that miR-608 overexpression in the OS cell lines and U2OS MG-63 inhibited cell proliferation and induced apoptosis. Furthermore, we demonstrated that macrophage migration inhibitory factor (MIF) was directly regulated by miR-608 which mediated the biological effects of miR-608 in OS. Restoration of MIF significantly reversed the inhibitory proliferation effect of miR-608. Taken together, our data provide compelling evidence that miR-608 functions as a tumour proliferation suppressor gene in OS by targeting MIF.

**Keywords:** MicroRNA-608, osteosarcoma, macrophage migration inhibitory factor, proliferation, apoptosis

## Introduction

Osteosarcoma (OS) has become the most common malignant bone in children and adolescents, and accounts for >10% of all solid tumour and 8.9% of cancer-related deaths in children [1]. OS is characterized by its highly metastatic features (particularly in the lung), which is a primary contributor to mortality in OS patients, and the early symptoms of OS are nonspecific, leading to a delay in early diagnosis [2]. Although the advances in diagnosis and appropriately systemic therapy, the overall 5-year survival rate has not been significantly improved due to the metastasis and recurrence of OS and chemoresistance [3]. The biological mechanisms underlying the initiation and progresses of OS remain poorly understood. Thus, it is an urgent need to optimise treatment strategies, identify biomarkers and explore new therapeutic agents for OS management.

MiRNAs are a class of endogenous, single-stranded, approximately 22 nucleotides non-

coding RNAs which regulate translation of their target genes by binding to complementary sequences in the 3'-untranslated region (3'UTR) of targeted messenger RNAs (mRNAs) [4]. MiRNAs are major factors in the genetic network that participate in pathophysiological processes, including the initiation and progression of cancers [5]. Recently, accumulating evidence that miRNAs can act as an oncogene or anti-oncogene in tumorigenesis, and aberrant regulation of miRNAs has been associated with various malignancies, such as gastric cancer [6], hepatocellular carcinoma [7], breast cancer [8] and colon cancer [9]. Moreover, emerging evidence shows that miRNAs play essential roles in controlling multiple steps of OS occurrence and development, including proliferation, apoptosis, invasion and metastasis [10-12].

The purpose of this study was to identify the role of miR-608 in OS tissue. In this study, we evaluated the clinical characteristics of miR-608 expression in OS tissue and provided evidence that miR-608 expression level was relat-

ed to the prognosis of OS patients. Our results demonstrated that introduction of miR-608 inhibited cell proliferation arrested cell cycle and induced cell apoptosis of OS cells by directly targeting MIF, indicating that miR-608 served as an anti-oncogene in OS pathology.

### Materials and methods

#### *Patients and tissue samples*

Human OS samples (n=82) and matched adjacent normal tissues were obtained from patients who underwent surgical resection at the Department of Orthopaedics, Wuxi Xishan People's Hospital between May 2013 and October 2014. Collected samples were flash frozen in liquid nitrogen and stored at -80°C for later RNA extraction or paraffin embedded for immunohistochemistry. All diagnoses were confirmed by an experienced pathologist. This study was approved by the Ethics Committee of Wuxi Xishan People's Hospital, and informed consent was obtained from all patients.

#### *RNA isolation and microRNA expression assay*

Total miRNAs were isolated using Trizol reagent (Invitrogen, Carlsbad, CA, USA) according to the manufacturer's instructions. Ten nanograms of total RNA was used for reverse transcription to cDNA with specific stem-loop real-time primers. Real-time polymerase chain reaction (qPCR) was performed using the SYBR Green Master Mix (Takara Bio Inc. Tokyo, Japan) on an ABI 7500 real-time PCR system (Applied Biosystems, Foster City, CA, USA). The relative quantification of miR-608 was calculated using the  $2^{-\Delta\Delta Ct}$  method. The data were normalized using U6 as an internal control.

#### *Cell culture and transfection*

The human OS cell lines U2OS and MG-63 were purchased from the Shanghai Institute of Cell Biology (CAS, Shanghai, China) and grown in Dulbecco's modified Eagle medium (DMEM, Invitrogen Life Technologies, Gaithersburg, MD, USA) supplemented with 10% foetal bovine serum (FBS, DMEM, Gibco Co., New York, USA) and 100 U/ml penicillin/streptomycin in humidified air at 37°C and 5% CO<sub>2</sub>. The miR-608 mimics and negative control mimics were purchased from RiboBio (Guangzhou, China). The cells were transfected with the miRNA mimics

at a final concentration of 50 nM using Lipofectamine 2000 reagent (Invitrogen) following the manufacturer's protocols. Cells were collected for further analyses performed 48 hours after transfection.

#### *Cell growth assay*

The cells were seeded into 96-well plates (1 × 10<sup>3</sup> cells/well) overnight. Then, cells were transfected with miR-608 or control mimics for 48 h. The cell viability was monitored using the Cell Counting Kit-8 (CCK-8, Dojindo, Kumamoto, Japan) at indicated time points (1, 2, 3, 4, 5 and 6 days after seeding into plates). The absorbance value in each well at 450 nm was measured with a Benchmark Microplate Reader (Bio-Rad Laboratories, Hercules, CA, USA).

#### *<sup>3</sup>H thymidine incorporation assay*

U2OS and MG-63 cells were plated onto 24-well plates at a density of approximately 4 × 10<sup>4</sup> cells/well and grown to 70%-80% confluence. Then, the cells were metabolically labelled with 1 μCi/mL <sup>3</sup>H thymidine (DuPont/NEN, Boston, MA, USA) for 4 h. The radioactivity was measured in a liquid scintillation counting system (Beckman Coulter, Fullerton, CA, USA).

#### *Cell cycle and cell apoptosis assay*

After 48 h transfection with miR-608 or control mimics, OS cells were collected by centrifugation, washed with cold phosphate buffered saline (PBS), fixed with 75% cold ethanol at -20°C overnight. The fixed cells were then washed with PBS, and stained with propidium iodide (Sigma-Aldrich, St. Louis, MO, USA) for 15 min. For the cell apoptosis assay, the cells were seeded into 6-well culture plates for 48 h after transfection and then harvested by trypsinization, washed with cold PBS and labelled by Annexin V FITC Apoptosis Detection kit (TIANGEN Biotech Co., Ltd., Beijing, China). Cell cycle distribution and the cell apoptosis rates were performed with BD Accuri C6 flow cytometry (Becton Dickinson, San Jose, CA).

#### *Transmission electron microscopy (TEM)*

The OS cells were fixed in ice-cold 2.5% glutaraldehyde, postfixed in 1% osmium tetroxide, dehydrated in graded alcohols, embedded in Epon 812, and cut into ultrathin sections. The

## MiR-608 suppresses osteosarcoma

sectioned were stained with uranyl acetate and lead citrate, followed by an examination using a JEM 1400 electron microscope (JEOL USA, Inc., Peabody, MA, USA) (80 kV).

### *Western blot assays*

Cells were lysed with ice-cold lysis RIPA buffer (ProMab Biotechnology, NY, USA) in the presence of Protease Inhibitor Cocktail (Pierce, Philadelphia, PA, USA). Protein concentration was quantified by the Bradford assay (Bio-Rad, Munich, Germany). Equivalent amounts of protein (30 µg) each was separated by 8% SDS-PAGE and transferred to nitrocellulose (NC) membrane (Bio-Rad, Munich, Germany). Membranes were blocked with 5% non-fat milk and incubated with primary antibodies overnight at 4°C and then incubated with the secondary antibodies for 2 h at room temperature. The bands were visualized with an Enhanced Chemiluminescence Kit (Beyotime, Shanghai, China) and exposure with an autoradiography film (Kodak, Shanghai, China). Rabbit polyclonal antibodies against MIF (Santa Cruz Biotechnology, Inc., Santa Cruz, CA). Mouse monoclonal antibody of GAPDH antibody (final dilution 1:1000, Cell Signaling Technology, Boston, USA) was used as a control.

### *Immunohistochemistry*

Formalin-fixed, paraffin embedded OS tissue specimens from patients were sectioned at 5 µm thick, deparaffinized in xylene and rehydrated in graded alcohol. An endogenous antigen-retrieval procedure was performed with 3% hydrogen peroxide in phosphate-buffered saline (PBS) for 10 min, and antigen-retrieved in a pressure cooker for 3 min in citrate buffer (pH 6.0). Subsequently, slides were incubated with monoclonal antibody to MIF (Santa Cruz Biotechnology, Santa Cruz, CA, USA) at 4°C in a humid chamber overnight. This was followed by incubation with biotinylated goat anti-rabbit immunoglobulin (Envision, Dako, Denmark) at a concentration of 1:200 for 30 min at 37°C. Then, antigen-antibody reaction was visualized with 3,3'-diaminobenzidine serving as the chromogen.

### *Plasmid construction*

The full-length 3'-untranslated region of MIF was cloned by PCR from MG63 cell cDNA library using primers as follow: MIF 3'UTR forward,

5'-GGGGTACCCAGAGCCGCAGGGACCCA-3', reverse, 5'-GAAGATCTTCAAGTCTCTAAACCGTTT-3'. For sequence point mutation, site-directed mutagenesis of potential target site in the MIF 3'UTR was performed using a QuikChange Site-Directed Mutagenesis kit (Promega, Madison, WI, USA). The PCR product was cloned into the KpnI and BglII restriction sites downstream of the luciferase open reading frame in the pGL3-promoter Luciferase vector (Ambion, Austin, TX, USA). MIF recombinant plasmid (lacking 3'UTR) was amplified by PCR from human cDNA library (MIF primers: forward, 5'-ATGCTCATCTGGGACTCTG-3' and reverse, 5'-TCAGCGGGGACATCCTGAGC-3'). The PCR amplicons of MIF were cloned into the T vector (Promega, Madison, WI, USA). The correct clones were confirmed by sequencing.

### *Luciferase reporter assays*

For luciferase assays, U2OS and MG-63 cells were grown to 70-80% confluence in 24-well plates and co-transfected with 100 ng firefly luciferase reporter vector containing the MIF 3'UTR or its mutant 3'UTR and 100 nM miR-608 or control mimics using Lipofectamine™ 2000 reagent (Invitrogen, Carlsbad, CA, USA) according to the manufacturer's instructions. Luciferase activity was analysed 48 h after co-transfection using dual luciferase assays (Promega, Madison, WI, USA) and the relative ratios were normalized against Renilla luciferase activity.

### *Statistical analysis*

All statistical analyses were performed using GraphPad Prism 5.0 (GraphPad Software, Inc., La Jolla, CA, USA). Values are shown as the mean ± standard deviation (SD). Significant differences were analysed using Student's t-test between two groups. Count data were analyzed by the Fisher's exact tests. Survival analysis was performed using Kaplan-Meier method and the Log-rank test. Differences were considered statistically significant at  $P < 0.05$ .

## **Results**

### *Downregulation of miR-608 expression in human OS tissues*

Expression level of miR-608 was detected in 82 pairs of OS tissues and adjacent normal tissues normalized to U6. To investigate associa-

## MiR-608 suppresses osteosarcoma

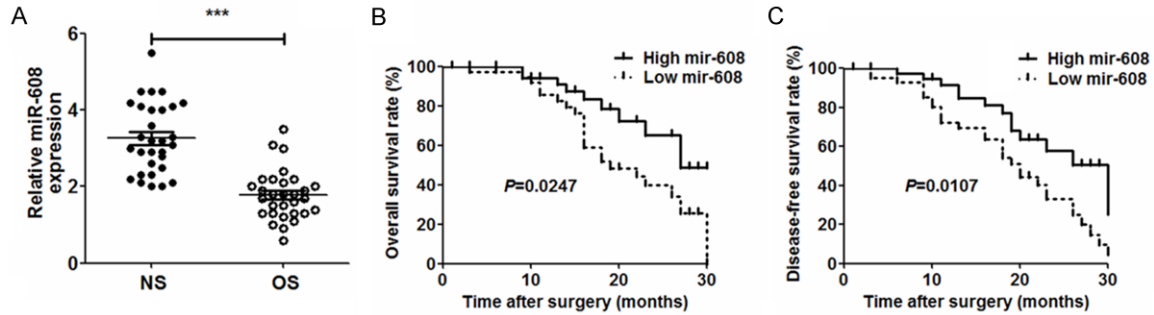


**Figure 1.** MiR-608 is downregulated in OS tissues. A. The relative expression of miR-608 in OS tissues and adjacent normal tissues was detected by qPCR. Kaplan-Meier curves of survival time in patients with OS divided according to miR-608 expression. B. Overall survival rate. C. Disease-free survival rate. Data are expressed as the mean  $\pm$  SD. \*\*\*,  $P < 0.001$ , vs. control group,  $n = 5$ .

**Table 1.** Correlations between miR-608 expression in osteosarcoma and clinical characteristics

Group	NO.	Relative miR-608 expression		P value
		Low	High	
Gender				
Male	42	19	23	0.5077
Female	40	22	18	
Age				
>18	34	17	17	1.0000
$\leq 18$	48	25	23	
Size of carcinoma (cm)				
>8	39	28	11	0.0003
$\leq 8$	43	13	30	
Histologic type				
Osteoblastic	26	15	11	0.5327
Chondroblastic	23	10	13	
Fibroblastic	19	8	11	
Telangiectatic	14	5	9	
TNM stage				
I stage	38	13	25	0.0005
II-IV stage	44	32	12	
Distant metastasis				
Negative	41	26	15	0.6507
Positive	41	24	17	

Based on the American Joint Committee on Cancer/International Union Against Cancer staging manual (2015).

tions of miR-608 expression with various clinicopathological parameters of OS patients, the 82 patients were divided into high miR-608 expression group and low miR-608 expression group using the median as a cutoff. As shown in **Figure 1**, miR-608 was significantly decreased in OS tissues compared with adjacent normal

tissues (**Figure 1A**). Furthermore, patients with high miR-608 expression had a significantly higher overall survival and disease-free survival rate than those with low miR-608 expression (**Figure 1B** and **1C**). The correlations of miR-608 expression with various clinicopathological parameters are summarized in **Table 1**. The results showed that there were significant correlations between miR-608 reduction and unfavourable variables, including carcinoma size ( $P = 0.0003$ ) and TNM stage ( $P = 0.0005$ ). No significant difference was observed between miR-608 expression and patients' gender, age, histologic type and distant metastasis.

### MiR-608 suppresses OS cell proliferation and induced cell apoptosis

To investigate cellular function of miR-608 in OS, miR-608 was overexpressed in human OS cells (U2OS and MG-63) by transfection with miR-608 mimics. Increased expression of miR-608 was confirmed by RT-PCR (**Figure 2A**). CCK-8 assay showed that miR-608 overexpression significantly inhibited the OS cell growth, and this effect increased with time (**Figure 2B**). Consistent with this result, the  $^3\text{H}$  thymidine incorporation assays also showed that miR-608 mimics significantly inhibited DNA synthesis in OS cell (**Figure 2C**). Cell cycle assay showed that overexpression of miR-608 in OS cells decreased the percentage of S phase and led to  $G_1$  arrest (**Figure 2D**). We also investigate the effect of miR-608 on cell apoptosis and found that increased apoptotic bodies in OS cells transfected with miR-608 mimics compared to cells transfected with control mimics (**Figure 2E** and **2F**). In addition, flow cytometry

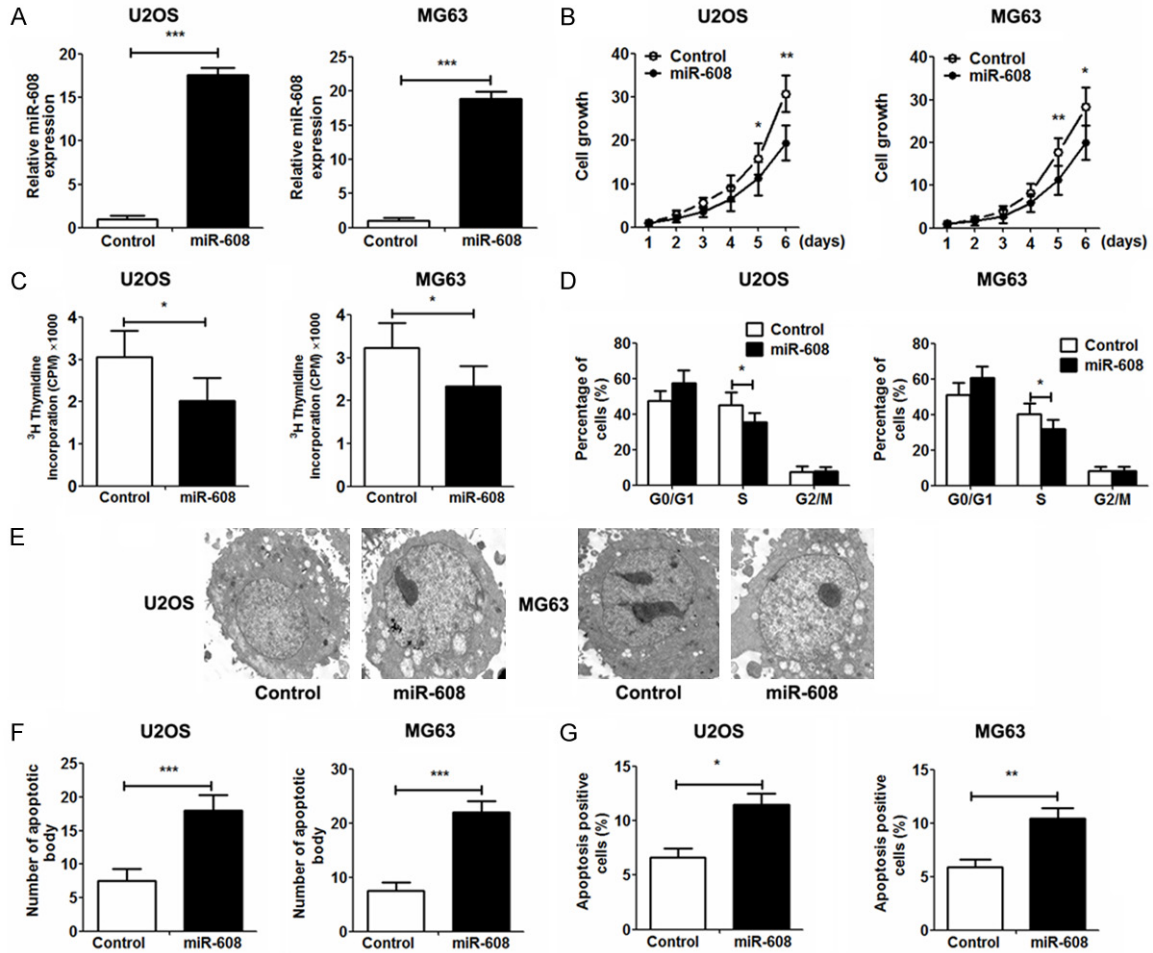


**Figure 2.** The effect of miR-608 on OS cell proliferation and apoptosis. A. Validation of miR-608 expression in U2OS and MG-63 cells by qPCR analysis. B. Cell growth curves for U2OS and MG-63 cells were measured by the CCK-8 assay. Absorbance on day 0 was assigned a value of 1. C. <sup>3</sup>H thymidine incorporation assays were performed to examine DNA synthesis. D. Frequencies of cells at different stages of the cell cycle. E. Representative images of TEM. F. The number of apoptotic body per cell was achieved by counting 5 high-power fields. G. The rate of cell apoptosis. Data are expressed as the mean ± SD. \*, P<0.05; \*\*, P<0.01; \*\*\*, P<0.001, vs. control group, n=5.

assay showed that cell apoptosis ratio significantly enhanced in OS cells transfected with miR-608 mimics (Figure 2G).

*MIF is a direct target of miR-608 in OS cells*

To explore the potential target of miR-608, two computational algorithms (TargetScan and miRanda) were used to identify miR-608 targets, and MIF was identified as potential target gene of miR-608. To demonstrate whether MIF is regulated by miR-608 in OS, we first examined the correlation between MIF and miR-608 expression in OS tissue specimens. Immunohistochemistry analysis showed that the expression of MIF levels in OS tissue with high miR-608 expression was significantly lower than those with low miR-608 expression (Figure

3A). Western blot analysis showed that overexpression of miR-608 significantly suppressed the expression of MIF protein in OS cells (Figure 4B). To verify whether miR-608 directly bind 3'UTR of MIF in OS cells, we synthesized the potential seed sequence for miR-608 in the 3'UTR region of MIF and cloned the wild type and mutant MIF 3'UTR fragments into a luciferase reporter gene system (Figure 3C). Luciferase reporter assay confirmed that the miR-608 had an obvious inhibitory effect on the wild-type (Wt) but not the mutant (Mut) 3'UTR of MIF luciferase activity (Figure 3D).

*Restoration of MIF reverses the effects of miR-608 in OS cells*

To determine whether miR-608 repression of OS cell growth was mediated by MIF, U2OS and

## MiR-608 suppresses osteosarcoma

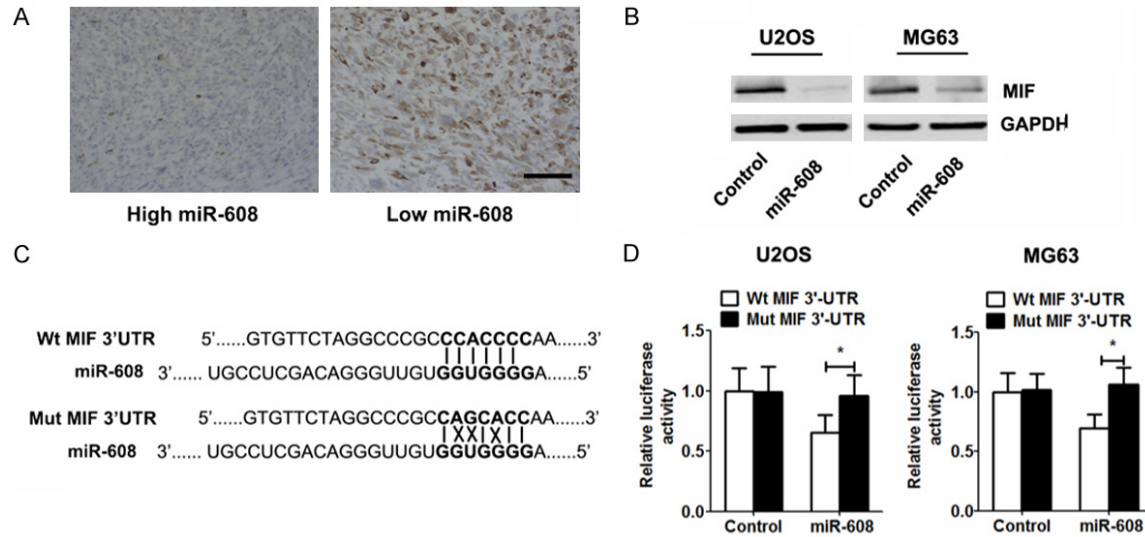


**Figure 3.** MiR-608 negatively regulates MIF expression in OS cells. A. Immunohistochemistry showed an inverse relationship between the expression of miR-608 and MIF in OS specimens (scale bar =100  $\mu$ m). B. Western blot was performed to detect MIF protein expression in OS cells. C. The predicted binding sites between miR-608 and the 3'UTR sequence of MIF is shown. D. Luciferase reporter assays in OS cells cotransfected with wild type 3'UTR MIF reporter plasmid or mutant type 3'UTR MIF, along with miR-608 or control mimics. The data are expressed as the mean  $\pm$  SD. \*,  $P < 0.05$ , vs. control group,  $n = 5$ .

MG-63 cells were transfected with MIF overexpression plasmid and empty vector. Western blot analysis demonstrated increased expression of MIF proteins in the OS cells transfected with this MIF construct compared with those transfected with the empty vector (**Figure 4A**). CCK-8 assay and  $^3\text{H}$  thymidine incorporation assay showed that re-expression of MIF exhibited an apparent rescue of OS cell proliferation (**Figure 4B** and **4C**). Flow cytometry and TEM assays showed that restoration of MIF abolished miR-608-induced  $G_1$ -S transition block and cell apoptosis in OS cells (**Figure 4D-F**).

### Discussion

The miRNAs have been reported as important regulators involved in various biological processes [13]. Therefore, identification of these small, non-coding RNAs and their targets involved in tumour pathology would provide valuable insight for the diagnosis and therapy of patients with human malignancies. Over the past decades, increasing studies have indicated that aberrant expression of miRNAs in cancer is not just a random event, but rather a programmed process in tumourigenesis [14]. Recently, it has been reported that miRNAs play a pivotal role in the initiation and development of OS [15].

MiR-608 has been deemed a novel prognostic marker in carcinogenesis, as demonstrated by the observation that downregulation of the miR-608 has frequently been detected in various tumours, including colon cancer [16], hepatocellular carcinoma [17] and chordoma cancer [18]. Our study indicated that miR-608 expression was downregulated in OS tissue relative to matched normal tissue, and its expression was significantly correlated with tumour size and TNM stage. Patients with lower levels of miR-608 tended to exhibit lower overall survival and disease-free survival rate than those with high miR-608 expression. In addition, introduction of miR-608 in OS cells remarkably suppressed proliferation and upregulated apoptosis. These results were consistent with previous studies demonstrating that miR-608 suppressed the tumourigenesis of various cancer cells in vitro and in vivo by targeting target gene and thereby suppressed cell proliferation, migration, and cell-cycle progression, as well as promoted apoptosis in tumour cells. Our data first revealed miR-608 acts as a tumour-suppressive gene in OS pathogenesis.

In addition, we confirmed that miR-608 was direct target gene of MIF, and we found that miR-608 negatively regulated MIF expression by directly targeting the 3'UTR of MIF mRNA in

## MiR-608 suppresses osteosarcoma

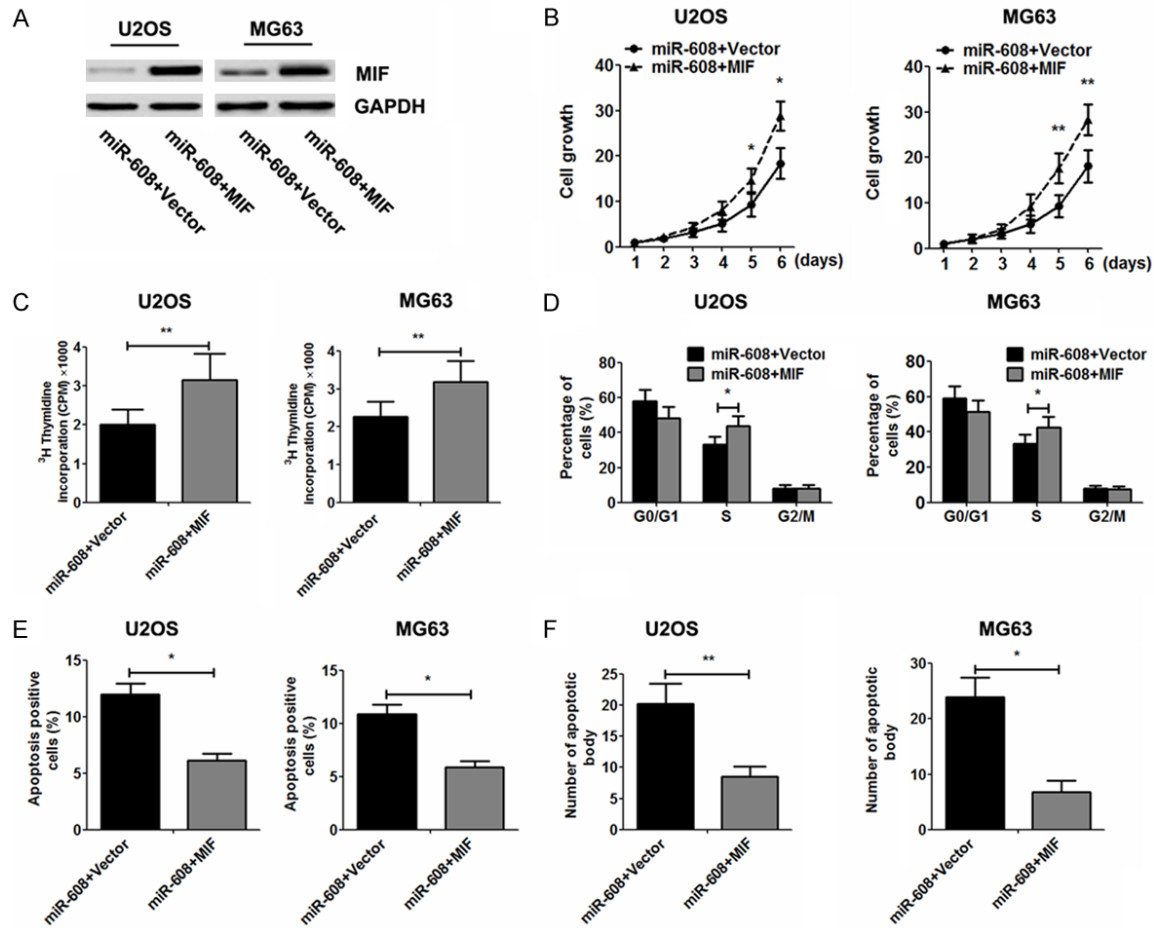


**Figure 4.** Restoration of MIF reverses the effect of miR-608 in OS cells. A. The expression of MIF protein was detected by Western blot. B. Cell growth curves for OS cells were measured by the CCK-8 assay. C. DNA synthesis was examined by <sup>3</sup>H thymidine incorporation assay. D, E. Cell cycle and cell apoptosis were analysed by flow cytometry. F. Quantification of the number of apoptotic body per cell. The data are expressed as the mean ± SD. \*, *P*<0.05; \*\*, *P*<0.01, vs. miR-608 + Vector group, n=5.

OS cells. MIF, originally described as a T cell-derived lymphokine, exhibits a broad range of immunostimulatory and proinflammatory activities [19]. MIF displays a dominant role in diseases that are characterized by pro-inflammatory pathways and plays a bridging role between inflammation and tumorigenesis [20]. Accumulating evidence reveal that MIF contributes to multiple aspects of tumour progression in several types of malignancies, including cell proliferation, survival, invasion of normal tissue, and tumour-associated angiogenesis [21-23]. Previous data clarify the prognostic role of MIF in predicting survival in osteosarcoma [24]. Recent studies have provided direct evidence that MIF was upregulated in osteosarcoma, and knockdown of MIF blocked osteosarcoma cell proliferation and invasion via inhibiting

angiogenesis [25]. Current study supports that MIF overexpression is a notable feature and may be one of the many critical events that occur in OS tumourigenesis.

Emerging evidence shows that the miRNAs moderate initiation and progression of several cancers by directly targeting MIF [26-28]. Recent study give a direct evidence that miR-608 exerts its anti-proliferation effect by directly targeting MIF in hepatocellular carcinoma cells [17]. In the current study, we validated MIF as a direct target gene for miR-608 in OS cells. In addition, we demonstrated that the inhibitory effect of miR-608 on proliferation and apoptosis could be reversed by re-expressing MIF, suggesting that miR-608 inhibited OS tumourigenesis by suppressing MIF expression.

In summary, our results indicated that down-regulation of miR-608 is significantly associated with larger tumour size, higher TNM stage and poor survival in patients with OS. Our data revealed the important molecular mechanism by which miR-608 inhibits proliferation and induced apoptosis in human OS cells by using concomitant suppression of MIF. This newly identified target of miR-608/MIF axis may be employed as a prognostic marker and therapeutic target for OS patients.

### Disclosure of conflict of interest

None.

**Address correspondence to:** Gonglian Liu and Huizhu Song, Department of Pharmacy, Wuxi People's Hospital Affiliated to Nanjing Medical University, 299 Qingyang Road, Wuxi 214023, China. Tel: +86-510-85151489; E-mail: gonglianliu@qq.com (GLL); Tel: +86-510-85151466; E-mail: huizhusong@qq.com (HZS)

### References

- [1] Mirabello L, Troisi RJ and Savage SA. Osteosarcoma incidence and survival rates from 1973 to 2004: data from the Surveillance, Epidemiology, and End Results Program. *Cancer* 2009; 115: 1531-1543.
- [2] Salinas-Souza C, De Oliveira R, Alves MT, Garcia Filho RJ, Petrilli AS and Toledo SR. The metastatic behavior of osteosarcoma by gene expression and cytogenetic analyses. *Hum Pathol* 2013; 44: 2188-2198.
- [3] Pierz KA, Womer RB and Dormans JP. Pediatric bone tumors: osteosarcoma ewing's sarcoma, and chondrosarcoma associated with multiple hereditary osteochondromatosis. *J Pediatr Orthop* 2001; 21: 412-418.
- [4] Mei Q, Li X, Guo M, Fu X and Han W. The miRNA network: micro-regulator of cell signaling in cancer. *Expert Rev Anticancer Ther* 2014; 14: 1515-1527.
- [5] Kloosterman WP and Plasterk RH. The diverse functions of microRNAs in animal development and disease. *Dev Cell* 2006; 11: 441-450.
- [6] Yan W, Qian L, Chen J, Chen W and Shen B. Comparison of Prognostic MicroRNA Biomarkers in Blood and Tissues for Gastric Cancer. *J Cancer* 2016; 7: 95-106.
- [7] Mizuguchi Y, Takizawa T, Yoshida H and Uchida E. Dysregulated microRNAs in progression of hepatocellular carcinoma: A systematic review. *Hepatol Res* 2015; [Epub ahead of print].
- [8] Wang J, Yang M, Li Y and Han B. The Role of MicroRNAs in the Chemoresistance of Breast Cancer. *Drug Dev Res* 2015; 76: 368-374.
- [9] Hollis M, Nair K, Vyas A, Chaturvedi LS, Gambhir S and Vyas D. MicroRNAs potential utility in colon cancer: Early detection, prognosis, and chemosensitivity. *World J Gastroenterol* 2015; 21: 8284-8292.
- [10] Liu Y, Li Y, Liu J, Wu Y and Zhu Q. MicroRNA-132 inhibits cell growth and metastasis in osteosarcoma cell lines possibly by targeting Sox4. *Int J Oncol* 2015; 47: 1672-1684.
- [11] Cheng DD, Yu T, Hu T, Yao M, Fan CY and Yang QC. MiR-542-5p is a negative prognostic factor and promotes osteosarcoma tumorigenesis by targeting HUWE1. *Oncotarget* 2015; 6: 42761-42772.
- [12] Liu X, Liang Z, Gao K, Li H, Zhao G, Wang S and Fang J. MicroRNA-128 inhibits EMT of human osteosarcoma cells by directly targeting integrin alpha2. *Tumour Biol* 2016; 37: 7951-7.
- [13] Li H, Zhang K, Liu LH, Ouyang Y, Guo HB, Zhang H, Bu J and Xiao T. MicroRNA screening identifies circulating microRNAs as potential biomarkers for osteosarcoma. *Oncol Lett* 2015; 10: 1662-1668.
- [14] Soifer HS, Rossi JJ and Saetrom P. MicroRNAs in disease and potential therapeutic applications. *Mol Ther* 2007; 15: 2070-2079.
- [15] Nugent M. microRNA and Bone Cancer. *Adv Exp Med Biol* 2015; 889: 201-230.
- [16] Yang H, Li Q, Niu J, Li B, Jiang D, Wan Z, Yang Q, Jiang F, Wei P and Bai S. microRNA-342-5p and miR-608 inhibit colon cancer tumorigenesis by targeting NAA10. *Oncotarget* 2016; 7: 2709-20.
- [17] Wang K, Liang Q, Wei L, Zhang W and Zhu P. MicroRNA-608 acts as a prognostic marker and inhibits the cell proliferation in hepatocellular carcinoma by macrophage migration inhibitory factor. *Tumour Biol* 2016; 37: 3823-30.
- [18] Zhang Y, Schiff D, Park D and Abounader R. MicroRNA-608 and microRNA-34a regulate chordoma malignancy by targeting EGFR, Bcl-xL and MET. *PLoS One* 2014; 9: e91546.
- [19] Leng L and Bucala R. Macrophage migration inhibitory factor. *Crit Care Med* 2005; 33: S475-477.
- [20] Liu Y, Zhao L, Ju Y, Li W, Zhang M, Jiao Y, Zhang J, Wang S, Wang Y, Zhao M, Zhang B and Zhao Y. A novel androstenedione derivative induces ROS-mediated autophagy and attenuates drug resistance in osteosarcoma by inhibiting macrophage migration inhibitory factor (MIF). *Cell Death Dis* 2014; 5: e1361.
- [21] Hira E, Ono T, Dhar DK, El-Assal ON, Hishikawa Y, Yamanoi A and Nagasue N. Overexpression of macrophage migration inhibitory factor in-

## MiR-608 suppresses osteosarcoma

- duces angiogenesis and deteriorates prognosis after radical resection for hepatocellular carcinoma. *Cancer* 2005; 103: 588-598.
- [22] Nishihira J, Ishibashi T, Fukushima T, Sun B, Sato Y and Todo S. Macrophage migration inhibitory factor (MIF): Its potential role in tumor growth and tumor-associated angiogenesis. *Ann N Y Acad Sci* 2003; 995: 171-182.
- [23] Ren Y, Tsui HT, Poon RT, Ng IO, Li Z, Chen Y, Jiang G, Lau C, Yu WC, Bacher M and Fan ST. Macrophage migration inhibitory factor: roles in regulating tumor cell migration and expression of angiogenic factors in hepatocellular carcinoma. *Int J Cancer* 2003; 107: 22-29.
- [24] Cates JM, Friedman DB, Seeley EH, Dupont WD, Schwartz HS, Holt GE, Caprioli RM and Young PP. Proteomic analysis of osteogenic sarcoma: association of tumour necrosis factor with poor prognosis. *Int J Exp Pathol* 2010; 91: 335-349.
- [25] Han I, Lee MR, Nam KW, Oh JH, Moon KC and Kim HS. Expression of macrophage migration inhibitory factor relates to survival in high-grade osteosarcoma. *Clin Orthop Relat Res* 2008; 466: 2107-2113.
- [26] Liu Z, Miao T, Feng T, Jiang Z, Li M, Zhou L and Li H. miR-451a Inhibited Cell Proliferation and Enhanced Tamoxifen Sensitive in Breast Cancer via Macrophage Migration Inhibitory Factor. *Biomed Res Int* 2015; 2015: 207684.
- [27] Liu N, Jiang N, Guo R, Jiang W, He QM, Xu YF, Li YQ, Tang LL, Mao YP, Sun Y and Ma J. MiR-451 inhibits cell growth and invasion by targeting MIF and is associated with survival in nasopharyngeal carcinoma. *Mol Cancer* 2013; 12: 123.
- [28] Bandres E, Bitarte N, Arias F, Agorreta J, Fortes P, Agirre X, Zarate R, Diaz-Gonzalez JA, Ramirez N, Sola JJ, Jimenez P, Rodriguez J and Garcia-Foncillas J. microRNA-451 regulates macrophage migration inhibitory factor production and proliferation of gastrointestinal cancer cells. *Clin Cancer Res* 2009; 15: 2281-2290.